SIRT1 in Astrocytes Regulates Glucose Metabolism and Reproductive Function

Irene Choi,[1]* Emily Rickert,[2]* Marina Fernandez,[2] and Nicholas J. G. Webster[1,2,3]

[1]VA San Diego Healthcare System, San Diego, California 92161; [2]Department of Medicine, School of Medicine, University of California San Diego, La Jolla, California 92093; and [3]Moores Cancer Center, University of California San Diego, La Jolla, California 92093

ORCiD numbers: 0000-0002-3827-5750 (N. J. G. Webster).

Sirtuin 1 (Sirt1) is an NAD-dependent class III deacetylase that functions as a cellular energy sensor. In addition to its well-characterized effects in peripheral tissues, evidence suggests that SIRT1 in neurons plays a role in the central regulation of energy balance and reproduction, but no studies have addressed the contribution of astrocytes. We show here that overexpression of SIRT1 in astrocytes causes markedly increased food intake, body weight gain, and glucose intolerance, but expression of a deacetylase-deficient SIRT1 mutant decreases food intake and body weight and improves glucose tolerance, particularly in female mice. Paradoxically, the effect of these SIRT1 mutants on insulin tolerance was reversed, with overexpression showing greater insulin sensitivity. The mice overexpressing SIRT1 were more active, generated more heat, and had elevated oxygen consumption, possibly in compensation for the increased food intake. The female overexpressing mice were also more sensitive to diet-induced obesity. Reproductively, the mice expressing the deacetylase-deficient SIRT1 mutant had impaired estrous cycles, decreased LH surges, and fewer corpora lutea, indicating decreased ovulation. The GnRH neurons were responsive to kisspeptin stimulation, but hypothalamic expression of *Kiss1* was reduced in the mutant mice. Our results showed that SIRT1 signaling in astrocytes can contribute to metabolic and reproductive regulation independent of SIRT1 effects in neurons. **(*Endocrinology* 160: 1547–1560, 2019)**

Sirtuin 1 (Sirt1) was first identified as a mammalian homolog of the yeast silent information regulator 2 (Sir2) protein, which is essential for lifespan extension due to caloric restriction. The sirtuins are class III histone deacetylases that need NAD+ for enzyme activity (1), and these enzymes function as cellular energy sensors sensitive to the intracellular NAD+/NADH ratio. Sirt1 is activated during fasting or caloric restriction to increase fatty acid oxidation and gluconeogenesis and suppress insulin secretion, insulin action, and adipogenesis (1–3). SIRT1 is ubiquitously expressed and has many important functions in peripheral metabolic tissues, including adipose tissue, liver, and muscle, that underlie its role in sensing energy balance (2, 4–6). Global knockouts are difficult to interpret because most mice die *in utero* or perinatally (7–9), and loss of the deacetylase enzyme activity mimics many of the effects of the knockout (10–12), suggesting that the majority, but not all, of SIRT1 function is related to its enzyme activity. Reproduction is a very energy-demanding process, so it is repressed under conditions of negative energy balance that may be triggered by famine, eating disorders such as anorexia and bulimia, and prolonged high-intensity exercise in humans (13, 14). A role for SIRT1 in regulating reproduction has been postulated, but conflicting results have been obtained. SIRT1 is expressed in spermatogonia and is necessary for normal spermatogenesis in males (15, 16). In females, SIRT1 is expressed in large ovarian

ISSN Online 1945-7170

Received 19 March 2019. Accepted 19 April 2019.
First Published Online 25 April 2019

*I.C. and E.R. should be considered co-first authors.

Abbreviations: AgRP, Agouti-related peptide; CON, wild-type control; DIO, diet-induced obesity; FBG, fasting blood glucose; FI, fasting insulin; GC, granulosa cell; GTT, glucose tolerance test; HFD, high-fat diet; HOMA-IR, homeostatic model assessment of insulin resistance; ITT, insulin tolerance test; LFD, low-fat diet; MUT, enzyme inactive mutant; NF-κB, nuclear factor κB; OX, SIRT1 overexpressing; POMC, pro-opiomelanocortin; qPCR, quantitative PCR; RER, respiratory exchange ratio; Sir2, silent information regulator 2; Sirt1, sirtuin 1; TAM, tamoxifen.

follicles, particularly in the oocyte and granulosa cells, and loss of SIRT1 causes small ovaries with early-stage follicular development but no evidence of ovulation (8, 17).

SIRT1 also plays a central role in preventing neuronal injury in ischemic stroke, Alzheimer's disease, brain injury, and neurodegeneration, possibly by reducing neuroinflammation (18–22), and SIRT1 expression and activity increase in the hypothalamus with fasting (23–25). Brain-specific deletion of *Sirt1* in progenitor cells using Nestin-cre decreases anxiety and depressive-like behavior (19, 21). We recently reported that overexpression of SIRT1 in neurons impaired ovulation and estrous cycles, consistent with reproductive suppression, but impaired rather than increased glucose tolerance (26). Expression of the deacetylase-deficient SIRT1 mutant had the opposite effects and was consistent with a previous report that loss of SIRT1 deacetylase function in neurons increased hypothalamic insulin signaling and improved peripheral insulin sensitivity. Genetic manipulation of Sirt1 in specific neurons has produced conflicting results. Deletion of Sirt1 in pro-opiomelanocortin (POMC) neurons decreases energy expenditure and increases susceptibility to diet-induced obesity (DIO) in mice (27), but deletion in Agouti-related peptide (AgRP) neurons has the opposite effect, consistent with the opposing roles of these two neuronal populations (28, 29). Mice lacking Sirt1 in *Sf1*-expressing neurons have increased susceptibility to DIO and insulin resistance, primarily because of decreased energy expenditure and skeletal muscle insulin sensitivity, and transgenic overexpression prevents these effects (30). Thus, Sirt1 in different neuronal populations may play distinct and sometimes even opposing roles in the regulation of energy balance.

Glial cells make up 50% of the cells in the central nervous system, but their role in metabolic and reproductive regulation has been largely overlooked (31–33). Astrocytes, the most abundant glial cell, may play a passive role by clearing synaptic potassium and neurotransmitters and support neuronal function (34–36), but recent evidence has shown that astrocytes may also play an active role. Insulin signaling in astrocytes controls glucose-induced activation of POMC neurons (37), and leptin signaling in astrocytes controls feeding and obesity (38). Furthermore, astrocyte inflammation is involved in promoting weight gain after high-fat diet feeding because loss of nuclear factor κB (NF-κB) signaling reduces food intake and increases energy expenditure (39), and loss of peroxisome proliferator–activated receptor-γ signaling in astrocytes impaired glucose tolerance and caused hepatic steatosis (40). Astrocytes also contribute to reproductive regulation because they suppress postsynaptic currents in GnRH neurons (41); produce RFRP-3, which inhibits GnRH secretion and action (41–44); and modulate GnRH release in the median eminence (45–47).

Because SIRT1 has effects on neuroinflammation, we investigated the role of SIRT1 in astrocytes in metabolic and reproductive regulation. We created an inducible, conditional deletion of the SIRT1 deacetylase domain or conditional overexpression of wild-type SIRT1 in astrocytes by using a GFAP-Cre-ERT mouse and show that the metabolic effect of SIRT1 is similar in astrocytes and neurons, but the reproductive effect of SIRT1 in astrocytes is the opposite of that seen in neurons.

Methods

Animals

Mice having a tamoxifen (TAM)-inducible cre-recombinase under the control of the human GFAP promoter (GCTF-*cre*), which is expressed in astrocytes, were mated with mice containing homozygous exon 4 floxed Sirt1 or floxed-STOP Sirt1 alleles. The resulting heterozygous/cre+ mice were then backcrossed to the appropriate homozygous floxed Sirt1 mice. Expression of cre deletes exon 4 of SIRT1, which encodes the acetylase domain, creating functionally enzyme inactive mutant (MUT) mice from the floxed allele, or causes overexpression of wild-type SIRT1 by deletion of the transcriptional STOP sequence from the flox-STOP allele [SIRT1-overexpressing (OX) mice]. The floxed-exon 4 and floxed-STOP Sirt1 mice were on a C57BL/6 background, whereas the GCTF-cre mice were on a Balb/c background. With our breeding scheme the final MUT and OX mice would be 75% C57BL/6 and 25% Balb/c. Mice were housed in a 12-hour light, 12-hour dark cycle. Body weights were recorded weekly out to 90 days of age for both sexes. Males and females had access to standard chow and water *ad libitum*. Weaning and genotyping were performed at 21 days after birth. Genotyping was performed by PCR on mouse-tail DNA with the primers listed in an online repository (48). The MUT and OX mice were housed in the same cages as their littermate controls. Mouse procedures conformed to the Guide for Care and Use of Laboratory Animals of the US National Institutes of Health and were approved by the Animal Subjects Committee of the University of California, San Diego.

Induction of recombination

Mice were fed a TAM diet (400 mg TAM citrate per kg diet) (TD.07262; Harlan Laboratories, Madison, WI) for 2 weeks starting at 10 weeks of age to induce deletion in Cre+ mice (MUT and OX). Mice were then returned to a normal chow diet for another 2 weeks to allow the metabolism and excretion of TAM before experiments proceeded. Cre-negative littermates from either the MUT or OX breeding pairs were treated with TAM and used as controls for TAM effects (Cre−/Tam), and Cre-positive MUT or OX mice that did not receive TAM were used as controls for Cre effects (Cre+/no-Tam). Analysis of the data from the four control groups did not show any significant differences, so the data from these control groups from both genotypes were combined into a single wild-type control (CON) group.

Intraperitoneal glucose tolerance and insulin tolerance tests

Mice at 5 months of age were subjected to IP glucose tolerance test (GTT) and insulin tolerance test (ITT). Mice were fasted for 6 hours and then injected IP with glucose (1 g/kg body weight) or human insulin (Novolin R, 0.4 U/kg body weight). Tail vein blood glucose was measured with a glucose meter (OneTouch Ultra; Bayer HealthCare, Tarrytown, NY) at 0, 15, 30, 45, 60, 90, and 120 minutes after injection.

Puberty onset and estrous cycles

Vaginal smear cytology was used to determine the estrous cycle phases. For the estrous cycle assessment, 3-month-old female mice were examined by vaginal cytology daily for 6 weeks. Samples were taken in the morning, vaginal fluid was transferred onto a slide, and the slide was stained with methylene blue (0.5% methylene blue and 1.6% potassium oxalate in water) and then visualized under a light microscope to assess reproductive stage. A cycle was defined as a day of diestrus or metestrus, followed by a day of proestrus, then a day of estrus. The length of the cycle was defined as the number of days between successive days of proestrus in normal diestrus-proestrus-estrus cycles.

Gene expression

Total RNA was extracted from whole brain after euthanasia with RNA-Bee (Tel-Test Inc., Friendswood, TX) used according to the manufacturer's instructions. First-strand cDNA was synthesized with a High Capacity cDNA synthesis kit (Applied Biosystems, Waltham, MA). Targeted quantitative PCR (qPCR) assays were run in 20 μL triplicate reactions on an MJ Research Chromo4 instrument with iTaq SYBR Green supermix (Bio-Rad, Hercules, CA). For gene expression assays with 7-nL microfluidic arrays (Fluidigm, San Francisco, CA), mRNA was extracted with RNA-Bee as before, but it was further purified with RNA purification kits (RNeasy; Qiagen, Germantown, MD) according to the manufacturer's instructions. Custom qPCR primers for a panel of targets were designed and synthesized by Fluidigm for their BioMark™ HD System. Gene expression levels were calculated after normalization to the housekeeping gene *m36B4* or *Gapdh* via the $2^{-\Delta\Delta CT}$ method and expressed as relative mRNA levels compared with the control. Primers are listed in an online repository (48).

24-hour fast

At 5 months of age, individually housed mice on normal chow were fasted for 24 hours from 9:00 AM to 9:00 AM. Water was provided *ad libitum*. Body was weighed, food intake was measured, serum was collected, and glucose levels were monitored before and after the fast.

High-fat diet feeding

At 4 months of age, groups of MUT, OX, and CON mice were randomly assigned to a 60% high-fat diet (HFD) to create DIO or to a matched 10% low-fat diet (LFD) (D12492 and D12450B; Research Diets Inc., New Brunswick, NJ) for 10 weeks. Mice had *ad libitum* access to water. Major lipid components of the HFD are derived from lard and include 20% palmitic acid, 11% stearic acid, 34% oleic acid, and 29% linoleic acid, resulting in 32% saturated fat, 36% monounsaturated, and 32% polyunsaturated fat. Body weight and food intake data were recorded weekly.

Tissue collection and histology

Testes, ovaries, brain, pituitaries, and other tissues were harvested at euthanasia for both histology and RNA extraction. Testes were fixed in Bouin solution for 6 hours and ovaries in formalin for 24 hours, followed by washing in 70% ethanol. Paraffin-embedded sections (5 μm) were cut, dewaxed, and stained with hematoxylin and eosin. Follicle number and stage and corpora lutea number were counted on three to five sections from ovaries from four to five mice per group and are presented as mean number per ovary (49). Follicle stages were defined as follows: 1° as having a single layer of cuboidal granulosa cells (GCs), 2° as having two or more layers of cuboidal GCs but no antrum, early antral as having small patches of clear space between GCs, antral as having clearly defined antrum, and atretic as having irregular oocyte morphology. Ovarian sections examined were separated by 50 μm. Images were scanned on an Aperio ImageScope and analyzed with the Imagescope software (Leica, Buffalo Grove, IL).

Gonadotropin measurements

Blood was collected from the tail vein of males and from females at the beginning of diestrus, proestrus, estrus, and metestrus for hormone analysis. Plasma LH and FSH levels were measured by Luminex assay (catalog number RPT86K; Millipore Corp, Bedford, MA). Sensitivity of the assay is as follows: LH, 4.9 pg/mL, and FSH, 47.7 pg/mL, with an intra-assay coefficient of variation of 15%. After 6, 12, and 20 weeks on the diets, female mice were bled in the morning of diestrus and at the time of the proestrus surge. Plasma LH and FSH levels were measured by Luminex assay (catalog number MPTMAG-49K). Sensitivity of the assays was as follows: LH, 4.9 pg/mL, FSH, 24.4 pg/mL. To determine whether a mouse surged, diestrus values from all lines were averaged (240 pg/mL), and any value greater than two SDs above the average (>612 pg/mL) was considered a surge. For the GnRH and kisspeptin stimulation tests, tail vein blood was collected before and 10 minutes (for GnRH) or 20 minutes (for kisspeptin) after IP injection of 1 μg/kg GnRH or 30 nmol kisspeptin-10, and gonadotropins were measured.

Insulin, leptin, and steroid measurements

Animals were fasted for 6 hours. Glucose was measured with a glucose meter, blood drawn from the tail vein, and plasma obtained. Fasting insulin (FI) and leptin were measured with the Mouse Metabolic Kit from Meso Scale Discovery (catalog no. K15124C-2; MSD, Rockville, MD). Sensitivity of the assay was as follows: leptin, 43 pg/mL, insulin, 15 pg/mL; coefficient of variation 6% and 12%, respectively. Estrogen, progesterone, and testosterone were measured with a Custom Steroid Hormone Panel Kit (MSD). Sensitivity of the assay was as follows: estradiol 5 pg/mL, progesterone 70 pg/mL, testosterone 20 pg/mL, with coefficients of variation 7%, 15%, and 22%, respectively.

In vivo leptin sensitivity test

We measured food intake in individually housed mice injected IP with 0.5 mg/kg leptin (National Hormone and Peptide Program, Harbor–University of California, Los Angeles) at 12-hour intervals (6:00 AM and 6:00 PM) for a total of four consecutive doses. Food intake and body weight were measured for

2 days before injection, for the 2-day injection period, and for 3 days afterward. A week later, the same process was repeated except with PBS. Food intake after leptin injection was compared with food intake after injections of saline.

Metabolic assessment

Six female mice per group (OX and MUT), matched for body weight, were individually housed in a 12-chamber Clinical Laboratory Animal Monitoring System with controlled temperature, light, and feeding (Columbus Instruments, Columbus, OH). Oxygen uptake, carbon dioxide output, respiratory exchange ratio (RER), horizontal and vertical ambulatory movement, feeding, and drinking were measured over a 3-day period. Data from the first 12 hours during day 1 acclimation were excluded from further analyses.

Statistical analysis

Data were analyzed by one-way or two-way ANOVA, or Student *t* test as appropriate in Prism (Graph Pad, La Jolla, CA). Pairwise comparisons were performed via Tukey *post hoc* tests after the ANOVA. Normality was assessed by D'Agostino-Pearson omnibus normality test. Results are expressed as mean ± SEM and considered significant at $P < 0.05$. Statistical differences are depicted with asterisks as $^{*}P < 0.05$, $^{**}P < 0.01$, and $^{***}P < 0.001$. Supplemental material is provided in an online data repository (48).

Results

Astrocyte SIRT1 alters food intake and body weight

Body weight and food intake were monitored daily for 10 weeks starting at 13 weeks of age. The OX females were significantly heavier and the MUT significantly lighter than the CON female mice (Fig. 1A). The differences in body weight were associated with significant differences in food intake (Fig. 1A inset), with OX mice eating 50% more food and MUT eating 24% less food than CON. Like the females, the OX males were significantly heavier than CON mice, but the MUT mice were not significantly different from the CON male mice (Fig. 1B). The differences in body weight were again associated with significant but smaller differences in food intake (Fig. 1B inset). Because of these differences in body weight and food intake, we measured circulating leptin levels in 6-hour fasted mice. Leptin levels were not altered in female mice (48) but were significantly lower in MUT male mice (48). We performed leptin sensitivity tests to see whether leptin was able to suppress food intake. Female and male mice were injected with 0.5 mg/kg of leptin twice a day for 2 days and food intake measured. Data were normalized to the same mice receiving saline injections instead of leptin the next week. All mice were leptin sensitive, and no significant differences were observed between genotypes (48).

Astrocyte SIRT1 alters glucose and insulin tolerance

At 5 months of age, mice were subjected to intraperitoneal GTT and ITT. For both experiments, mice were fasted for 6 hours before the tests. During the GTT, OX females were significantly less glucose sensitive than CON mice, whereas the MUT mice were significantly more glucose sensitive than CON mice (Fig. 1C). The intolerance and sensitivity were confirmed by calculating the glucose excursion by area under the curve (Fig. 1C inset). Like the females, OX males were also glucose intolerant compared with CON males, but the MUT mice were indistinguishable from CON (Fig. 1D). The glucose intolerance in the OX males was confirmed by area under the curve (Fig. 1D inset). The body weights were no different between GTT groups for the males, but the females were significantly different (48). To eliminate any potential effect of body weight on glucose tolerance, a subset of females with equal body weight was compared, and the same differences in GTT were observed (48). Differences between the groups persisted if male and female results were combined (48). Insulin and C-peptide levels were measured in 6-hour fasted mice and compared with fasting blood glucoses (FBGs). FBGs were lower in MUT females and higher in OX males and females, as before (Fig. 1E and 1F). FI levels were unchanged in female mice, but the MUT male mice had lower FI levels (Fig. 1F). Homeostatic model assessment of insulin resistance (HOMA-IR) calculations showed that both female (Fig. 1E) and male (Fig. 1F) MUT mice are insulin sensitive. The C-peptide measurements showed that insulin secretion is not altered between the genotypes (Fig. 1E and 1F), suggesting that differences in insulin levels are probably related to insulin clearance.

For the ITTs, the OX females had a significantly higher mean FBG that dropped to lower values than CON mice at 60 and 90 minutes (Fig. 2A). The MUT females had lower mean FBG than CON mice, but subsequent values were no different than those of CON mice (Fig. 2A). Similar effects were seen in male mice, with OX mice having higher mean FBG than CON or MUT mice and the values dropping more markedly at 30 to 90 minutes (Fig. 2B). Calculation of the area above the curve confirmed that the OX mice showed a greater drop in blood glucose (Fig. 2A and 2B insets). When the data were plotted as percentage basal, the female OX mice were significantly more insulin sensitive and the MUT significantly less sensitive than CON mice (Fig. 2C). The MUT males were no different from the CON males, as observed in the GTTs, but the OX males were significantly more insulin sensitive than either CON or MUT groups (Fig. 2D).

Because of the differences in food intake, we tested the expression of hypothalamic hormones involved in the

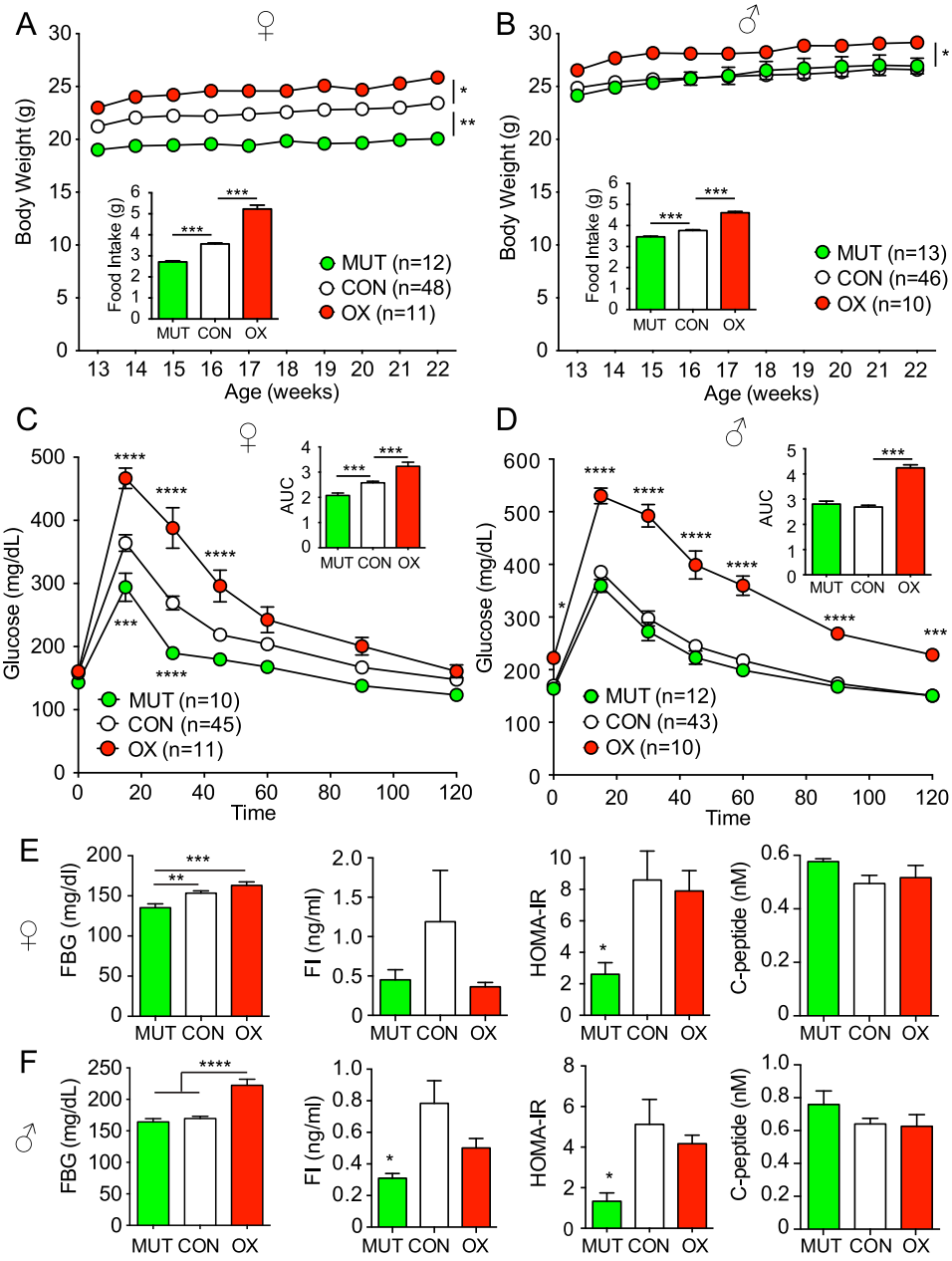

Figure 1. Overexpression of SIRT1 in astrocytes causes weight gain and glucose intolerance. (A) Body weights of female mice after TAM induction up to 22 weeks of age. OX mice are in red, CON mice in white, and MUT mice in green (n = 11, 48, and 12, respectively). Repeated-measures two-way ANOVA indicated a significant time effect ($P = 0.016$) and a significant genotype effect ($P < 0.0001$). Inset shows average daily food intake. (B) Body weights and average food intake for male mice up to 22 weeks of age (n = 10 for OX, n = 46 for CON, and n = 13 for MUT). Repeated-measures two-way ANOVA indicated a significant time effect ($P = 0.002$) and a significant genotype effect ($P < 0.0001$) for body weight. (C) GTTs performed in female mice at 3 months of age (n = 11 for OX, n = 45 for CON, and n = 10 for MUT). Repeated-measures two-way ANOVA indicated significant genotype and time effects and interaction ($P < 0.0001$). Inset shows area under the curve (AUC). (D) GTTs performed in male mice at 3 months of age (n = 10 for OX, n = 41 for CON, and n = 12 for MUT). Repeated-measures two-way ANOVA indicated significant genotype and time effects and interaction ($P < 0.0001$). Inset shows AUC. (E) FBG, FI, HOMA-IR, and C-peptide levels for 6-hour fasted female mice (n = 21 for OX, n = 22 for CON, n = 19 for MUT). (F) FBG, FI, HOMA-IR, and C-peptide levels for 6-hour fasted male mice. Results are presented as mean ± SEM. Asterisks indicate significance from *post hoc* testing. *$P < 0.05$; **$P < 0.01$; ***$P < 0.001$; ****$P < 0.0001$.

regulation of feeding in RNA extracted from whole brain. Neuropeptide Y (*Npy*) showed both a genotype and sex-dependent difference in expression by two-way ANOVA (Fig. 2E), with higher expression in OX mice. Agouti-related peptide (*Agrp*) also showed higher expression in OX males (Fig. 2E). The genes encoding two other orexigenic peptides, Orexin A (*Hcrt*) and Nesfatin (*Nucb2*), did not show any alterations (Fig. 2E). Expression of *Sirt1* was elevated in the female and male OX mice, as expected (48). We also observed changes in inflammatory gene expression. Expression of interleukin-6 (*Il6*) was reduced in female MUT mice but elevated in

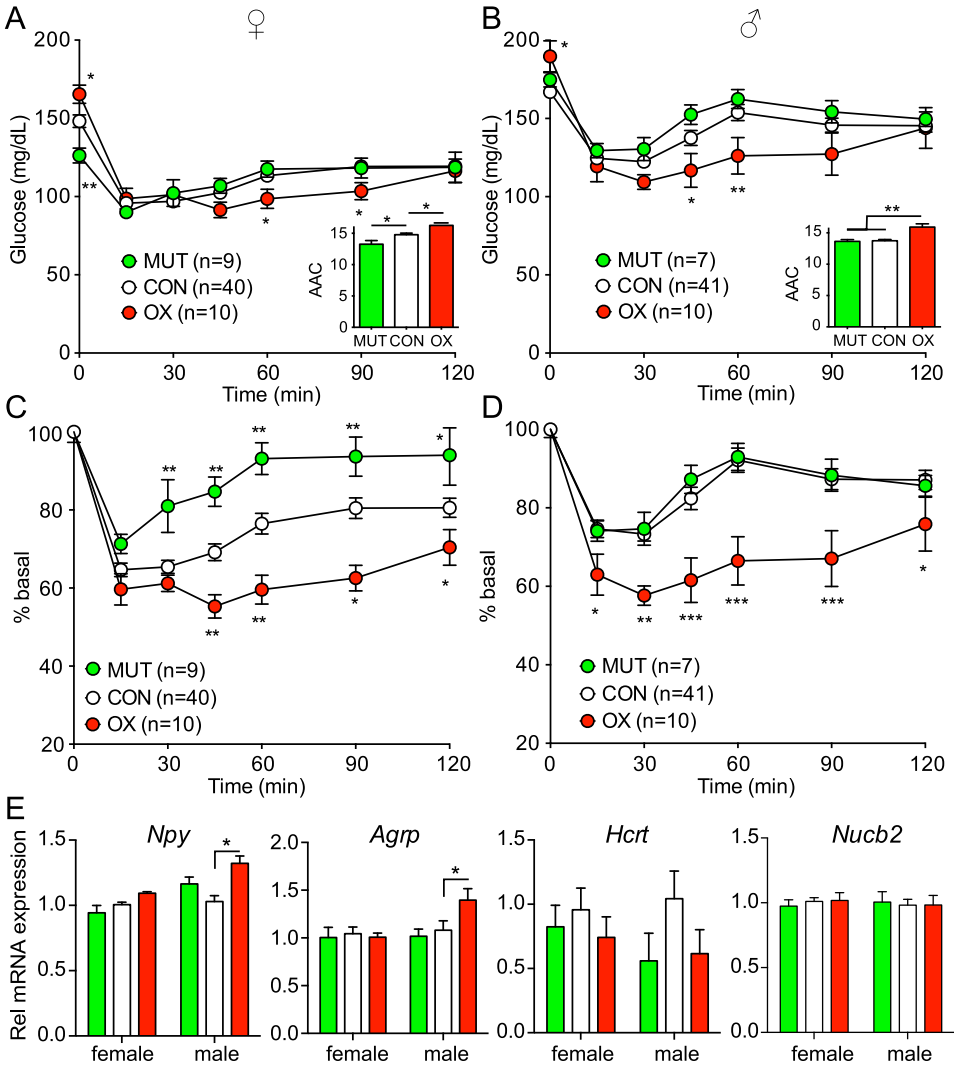

Figure 2. Overexpression of SIRT1 in astrocytes increases insulin sensitivity. (A) ITTs performed in female mice at 3 months of age (n = 9 for OX, n = 36 for CON, n = 9 for MUT). OX mice are in red, CON mice in white, and MUT mice in green. Repeated-measures two-way ANOVA indicated significant time effect and time-genotype interaction ($P < 0.0001$) but no genotype effect. Inset shows area above the curve (AAC). (B) ITTs performed in male mice at 3 months of age (n = 7 for OX, n = 39 for CON, n = 9 for MUT). Repeated-measures two-way ANOVA indicated significant time effect and genotype-time interaction ($P < 0.001$ and $P < 0.0001$) but no genotype effect. Inset shows AAC. (C) ITTs in female mice presented as percentage basal fasting glucose level. Repeated-measures two-way ANOVA indicated significant time effect and genotype effects ($P < 0.0001$) and interaction ($P < 0.001$). (D) ITTs in male mice presented as percentage basal fasting glucose level. Repeated-measures two-way ANOVA indicated significant time effect and genotype effects ($P < 0.0001$ and $P < 0.01$) and interaction ($P < 0.001$). (E) Hypothalamic orexigenic gene expression for neuropeptide Y (*Npy*), agouti-related peptide (*Agrp*), orexin-A (*Hcrt*), and nesfatin (*Nucb2*) in MUT, CON, and OX mice. Gene expression from female mice (n = 8 for MUT, n = 27 for CON, and n = 6 for OX) and male mice (n = 7 for MUT, n = 28 for CON, and n = 7 for OX) by qPCR. Results are presented as mean ± SEM. Asterisks indicate significance from *post hoc* testing. $*P < 0.05$; $**P < 0.01$; $***P < 0.001$.

male OX mice (48). The interleukin-12 p40 subunit (*Il12b*) was reduced in female MUT mice (48), but tumor necrosis factor α (*Tnfa*) was increased in male OX mice (48). The results are consistent with the increased feeding seen in the OX mice.

Mice overexpressing SIRT1 show altered activity during the dark phase

Because the OX mice were glucose intolerant and the MUT mice glucose sensitive, we subjected OX and MUT mice to a metabolic assessment with continuous monitoring over 3 days. Female mice (3 months old) were used for this experiment, because the MUT male mice did not have a glucose-sensitive phenotype. The mice were chosen to have the same body weight to eliminate body weight as a variable. The mice did not lose a significant amount of body weight during the study (48). The OX mice showed stronger diurnal changes in rearing and ambulatory activity (Fig. 3A and 3B) and showed an anticipatory increase in activity before the onset of the dark phase. When averaged over 12 hours, the OX mice showed greater activity in both the dark and light phases

(48). Interestingly, the cage temperature was elevated in the OX mice and did not show the normal diurnal changes (Fig. 3C), which may reflect the increased physical activity in the OX mice. The RER was unchanged between the genotypes (Fig. 3D), but the MUT mice have a significantly lower mean RER during the light phase (48), indicating that they are preferentially using oxidizing lipid. Oxygen consumption (VO_2) was significantly different between the genotypes, but carbon dioxide production (VCO_2) was not (Fig. 3E and 3F); both were lower in the OX mice during the light and dark phases (48). Mean food and water intake was not altered by genotype during the study (Fig. 3G and 3H). Thus the OX mice showed greater activity and heat generation that partially compensated for the elevated food intake.

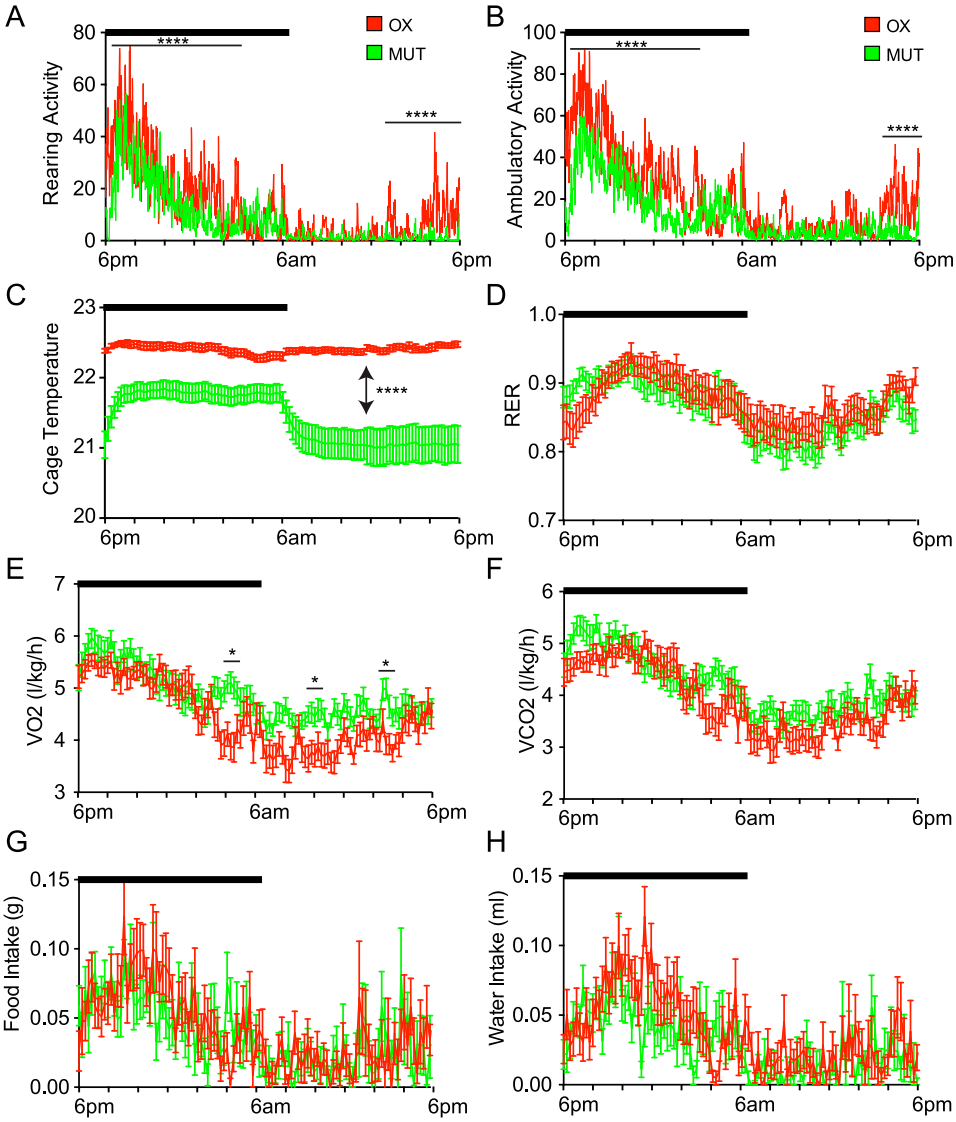

Figure 3. Metabolic cage studies of female OX and MUT mice. OX mice (n = 6) are shown in red and MUT mice (n = 6) in green. Graphs show diurnal patterns over 24 hours measured per minute for physical activity or per 13-minute interval for other measurements. Horizontal black bar indicates period of lights off (6:00 PM to 6:00 AM). Time of day is indicated on the *x*-axis. (A) Rearing activity over 24 hours. Repeated-measures two-way ANOVA indicated significant genotype and time effects ($P < 0.0001$) and interaction ($P < 0.0001$). (B) Ambulatory activity over 24 hours. Repeated-measures two-way ANOVA indicated significant genotype and time effects ($P < 0.0001$) and interaction ($P < 0.0001$). (C) Cage temperature over 24 hours. Repeated-measures two-way ANOVA indicated significant genotype and time effects ($P < 0.0001$) and interaction ($P < 0.0001$). (D) RER over 24 hours. Repeated-measures two-way ANOVA indicated significant time effect ($P < 0.0001$) and a significant interaction ($P < 0.0001$) but no genotype effect. (E) Volume O_2 consumed (VO2) over 24 hours. Repeated-measures two-way ANOVA indicated significant time ($P < 0.0001$) and genotype ($P < 0.01$) effects and a significant interaction ($P < 0.0001$). (F) Volume CO_2 produced (VCO2) over 24 hours. Repeated-measures two-way ANOVA indicated significant genotype ($P < 0.05$) and time effects ($P < 0.0001$) and interaction ($P < 0.01$) but no *post hoc* significant differences between genotypes. (G) Food intake over 24 hours. Repeated-measures two-way ANOVA indicated significant time effect ($P < 0.0001$) but no genotype effect or interaction. (H) Water intake over 24 hours. Repeated-measures two-way ANOVA indicated significant genotype and time effect ($P < 0.0001$), no genotype effect, but a significant interaction ($P < 0.01$). Results are presented as mean ± SEM. Asterisks indicate significant differences between genotypes after *post hoc* testing. *$P < 0.05$; ****$P < 0.0001$.

Astrocyte SIRT1 does not alter the response to a 24-hour fast

Because SIRT1 may play a role in the effects of calorie restriction, we tested whether the SIRT1 in astrocytes alters the response to fasting. Individually housed 5-month-old female (Fig. 4A–4C) and male (Fig. 4D–4F) mice were subjected to a 24-hour fast. Body weight, food intake, and blood glucose levels were measured 2 days before, during, and 2 days after the fast. All genotypes in both female and male mice showed a drop in body weight after the 24-hour fast that recovered within 24 hours (Fig. 4A and 4D). Differences in weights between the genotypes were maintained during the 24-hour fast. Glucose levels dropped equivalently during the 24-hour fast in both female and male mice but still showed the genotypic differences observed before (Fig. 4B and 4E). The glucose levels returned to normal 24 hours later. All mice showed the expected rebound eating for the first 24 hours after the fast, which returned to normal after 2 days (Fig. 4C and 4F). These results suggested that genetic manipulation of *Sirt1* in astrocytes did not alter the response to fasting.

Astrocyte SIRT1 causes more weight gain in female mice, but not male mice, on HFD

Although caloric restriction leads to an increase in SIRT1, HFD has been associated with low SIRT1 activity. So mice were randomly selected at 17 weeks of age for either an HFD (60 cal%) or a matched LFD (10 cal %). Body weight and food intake were measured weekly for 10 weeks, and mice were euthanized at 27 weeks. Females on the LFD maintained their body weight, although the OX females showed slightly greater separation from the other two genotypes (Fig. 4G). The weekly food intake reflected the difference in body weight (Fig. 4G inset). Females on the HFD showed significant differences in weight gain (Fig. 4H). After 4 weeks of HFD the OX females weighed significantly more than the MUT (Fig. 4H), and their weight continued to diverge from that of the CON mice over the next 6 weeks. The MUT mice initially gained weight at the same rate as the CON mice, but the weights started to diverge after 5 weeks, and the MUT mice gained less weight thereafter, although they had not reached significance at the end of the study (Fig. 4H). The differences in weight gain were again reflected in differences in food intake between the genotypes (Fig. 4G and 4H insets). No differences in body weight were observed for male mice on LFD or HFD (Fig. 4I and 4J), although there were small but significant differences in food intake between genotypes on HFD (Fig. 4G inset). These results indicated that astrocyte SIRT1 influenced the development of obesity in female mice.

Astrocyte SIRT1 promotes and lack of SIRT1 impairs estrus cycles

To evaluate the reproductive role of SIRT1 in astrocytes, estrous cycles were documented in postpubertal females, over the course of 6 weeks from 14 to 20 weeks of age. The OX mice showed a greater number of cycles during this period than MUT or CON mice (Fig. 5A), with more days in diestrus and fewer days in estrus compared with MUT mice (Fig. 5B). We measured FSH and LH levels at each estrous stage. No differences were seen at diestrus, early proestrus, or estrus between the genotypes (Fig. 5C). All genotypes showed an increase in LH during the afternoon of proestrus (Fig. 5D), but when mice were divided into those with a detectable LH surge and those without, significant differences in the number of surges were observed (Fig. 5D). Roughly 50% of the CON mice surged (11/24) but only 12% of the MUT mice (1 out of 7), and 88% of OX mice surged (7/8). The FSH values were also significantly different (Fig. 5E). The OX mice had lower FSH values in diestrus and early proestrus and showed a clear increase during late proestrus and estrus, whereas the MUT mice did not show a difference in FSH at any point of the cycle. The CON mice showed the expected increase in FSH during estrus.

Because the LH surge appeared to be impaired in MUT females, we performed a GnRH stimulation test. LH and FSH were measured before and 10 minutes after an IP injection of GnRH (1 μg/kg). The pituitary response was intact in all genotypes as the LH increased in response to the GnRH bolus (48). We verified this finding by repeating the experiment in male mice (48). FSH did not change in response to GnRH in any genotype or sex (48). We then tested whether the GnRH neurons were responsive by performing a kisspeptin stimulation test in female mice. LH and FSH were measured before and 20 minutes after an IP injection of kisspeptin 10 (30 nmol). All three genotypes showed the expected rise in LH (48), with no change in FSH (48).

We then tested the expression of hypothalamic hormones involved in the regulation of reproduction. Expression of the genes encoding kisspeptin (*Kiss1*) and RFRP3 (*Npvf*) were altered in MUT and OX female mice, but genes encoding GnRH (*Gnrh1*), oxytocin (*Oxt*), dynorphin (*Pdyn*), and neurokinin B (*Tac2*) were unchanged (Fig. 5F and 5G).

We assessed follicle development and ovulation by examining ovarian histology after euthanasia. The ovaries from MUT mice were significantly smaller than those of CON or OX mice (Fig. 6A and 6B) and had a lower number of antral follicles and corpora lutea and a higher number of atretic follicles (Fig. 6C) consistent

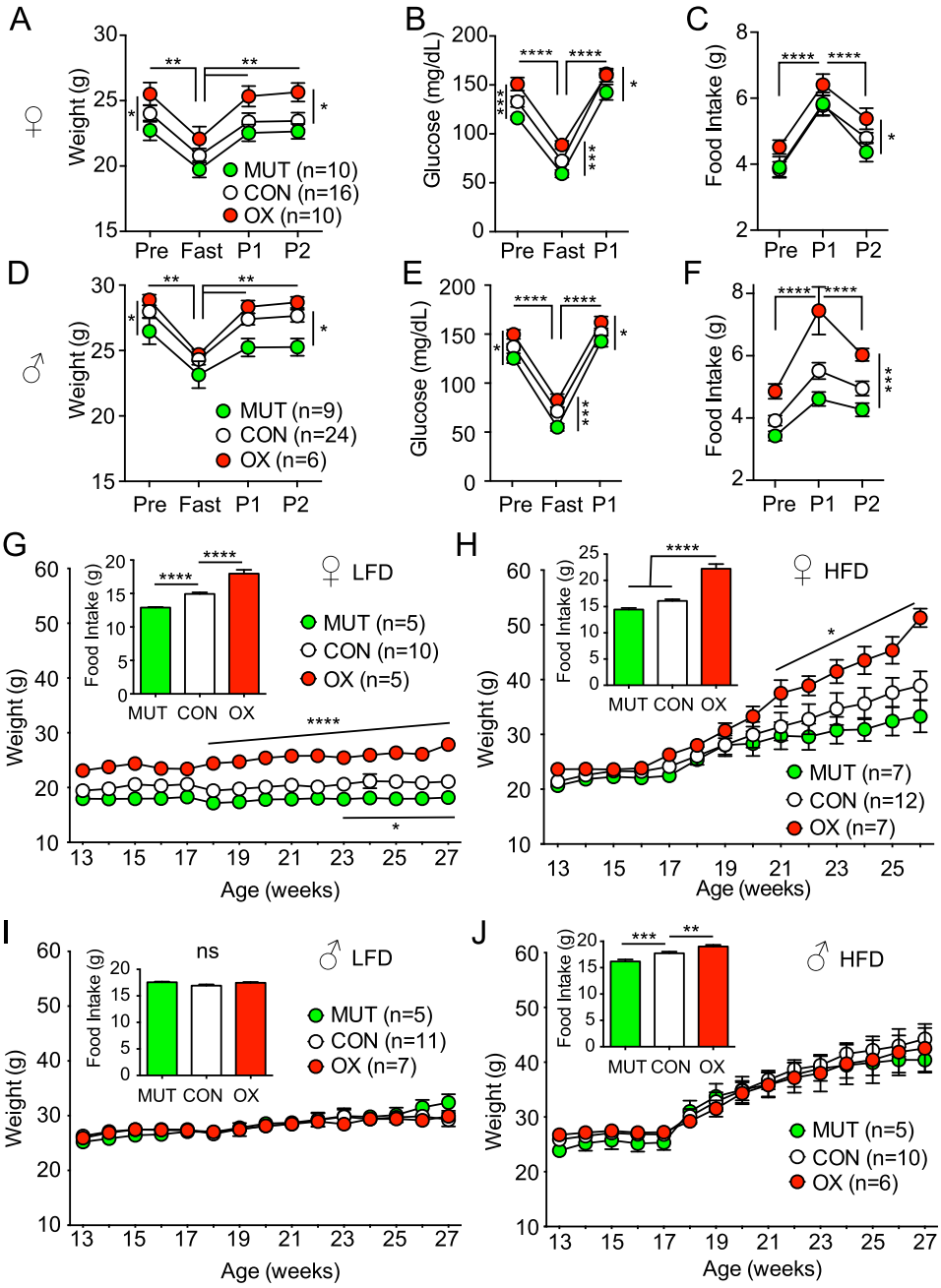

Figure 4. Overexpression of SIRT1 does not alter the response to fasting but increases weight gain in females on an HFD. OX mice are in red, CON mice in white, and MUT mice in green. (A) Body weight for female mice before, during, and after a 24-hour fast (n = 10 for OX, n = 16 for CON, n = 10 for MUT). (B) Blood glucose before, during, and after a 24-hour fast. (C) Food intake before and for 2 days after a 24-hour fast. (D) Body weight for male mice before, during, and after a 24-hour fast (n = 10 for OX, n = 16 for CON, n = 10 for MUT). (E) Blood glucose before, during, and after a 24-hour fast. (F) Food intake before and for 2 days after a 24-hour fast. Repeated-measures two-way ANOVA indicated significant time and genotype effects ($P < 0.0001$) for weight and blood glucose and a significant time effect ($P < 0.0001$) and genotype effect ($P < 0.05$) for food intake for both female and male mice. (G) Body weight of female mice on an LFD for 10 weeks (n = 5 for OX, n = 10 for CON, n = 5 for MUT). Repeated-measures two-way ANOVA indicated significant time and genotype ($P < 0.001$) effects. Inset shows mean daily food intake. (H) Body weight of female mice on an HFD for 10 weeks (n = 7 for OX, n = 12 for CON, n = 7 for MUT). Repeated-measures two-way ANOVA indicated significant time effect and genotype-time interaction ($P < 0.0001$). Inset shows mean daily food intake. (I) Body weight of male mice on an LFD for 10 weeks (n = 7 for OX, n = 11 for CON, n = 5 for MUT). Inset shows mean daily food intake. (J) Body weight of male mice on an HFD for 10 weeks (n = 6 for OX, n = 10 for CON, n = 5 for MUT). Repeated-measures two-way ANOVA indicated no significant time and genotype effects for weight on LFD or HFD for male mice. Inset shows mean daily food intake. Data are shown as mean ± SEM. Asterisks indicate significance by *post hoc* testing as indicated. *$P < 0.05$; **$P < 0.01$; ***$P < 0.001$; ****$P < 0.0001$.

with impaired follicle development and ovulation. Estrogen levels were unchanged in the female mice, and progesterone levels mirrored the LH surges, with lower levels in the MUT mice (Fig. 6D). No differences in testicular morphology were observed in the male mice (48).

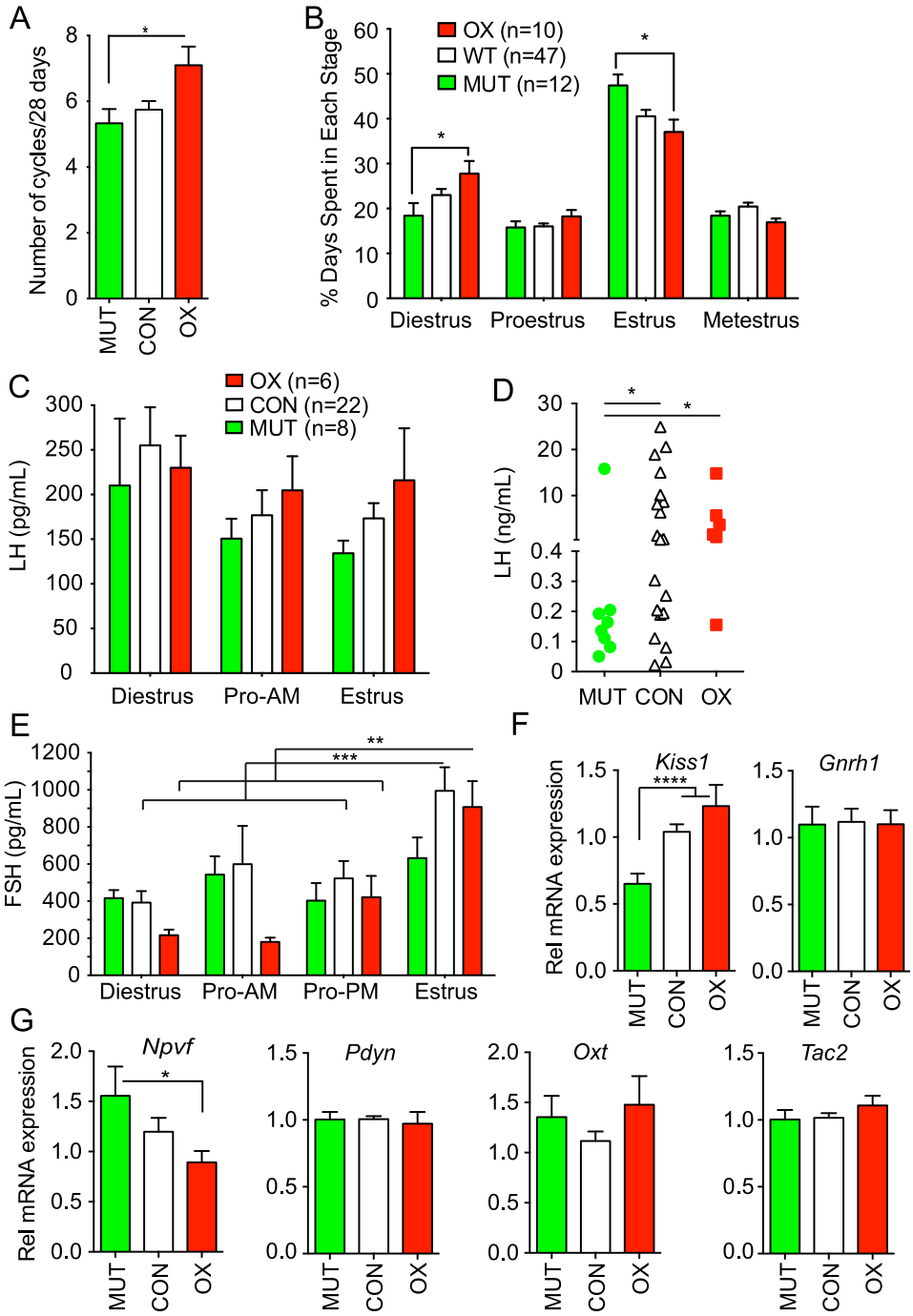

Figure 5. Overexpression of SIRT1 increases estrous cycling and ovulation in female mice. OX mice are in red, CON mice in white, and MUT mice in green. (A) Number of estrous cycles over 28 days of cycling by vaginal cytology (n = 10 for OX, n = 47 for CON, n = 12 for MUT). (B) Percentage of days spent in each stage of the estrous cycle over 28 days (n = 10 for OX, n = 47 for CON, n = 12 for MUT). Two-way ANOVA indicated significant stage effect ($P < 0.0001$) and significant interaction of stage and genotype ($P < 0.0001$). (C) LH levels during diestrus, the morning of proestrus, and the morning of estrus (n = 6 for OX, n = 20 for CON, n = 8 for MUT). Two-way ANOVA indicated no significant differences. (D) LH levels during the afternoon of proestrus (n = 6 for OX, n = 20 for CON, n = 8 for MUT). Asterisks indicate a significant difference in the number of LH surges by Fisher exact test. (E) FSH levels during diestrus, the morning of proestrus, the afternoon of proestrus, and the morning of estrus (n = 6 for OX, n = 20 for CON, n = 8 for MUT). Two-way ANOVA indicates significant stage effect ($P = 0.002$) but no significant genotype effect or interaction. (F) Hypothalamic *Kiss1* and *Gnrh1* expression in MUT, CON, and OX mice by qPCR. (G) Hypothalamic neuropeptide gene expression for MUT, CON, and OX mice by qPCR. n = 8 for MUT. n = 27 for COM, n = 6 for OX for qPCR data. Results are presented as mean ± SEM. Asterisks indicate significance from *post hoc* testing as indicated. *$P < 0.05$; **$P < 0.01$; ***$P < 0.001$; ****$P < 0.0001$.

Discussion

Previously, loss of SIRT1 enzyme activity in neurons did not alter glucose metabolism in male mice but increased insulin sensitivity in the brain and periphery and partially protected mice from HFD-induced obesity (50). In female mice we observed that similar loss of SIRT1 enzyme activity in neurons improved glucose tolerance by GTT.

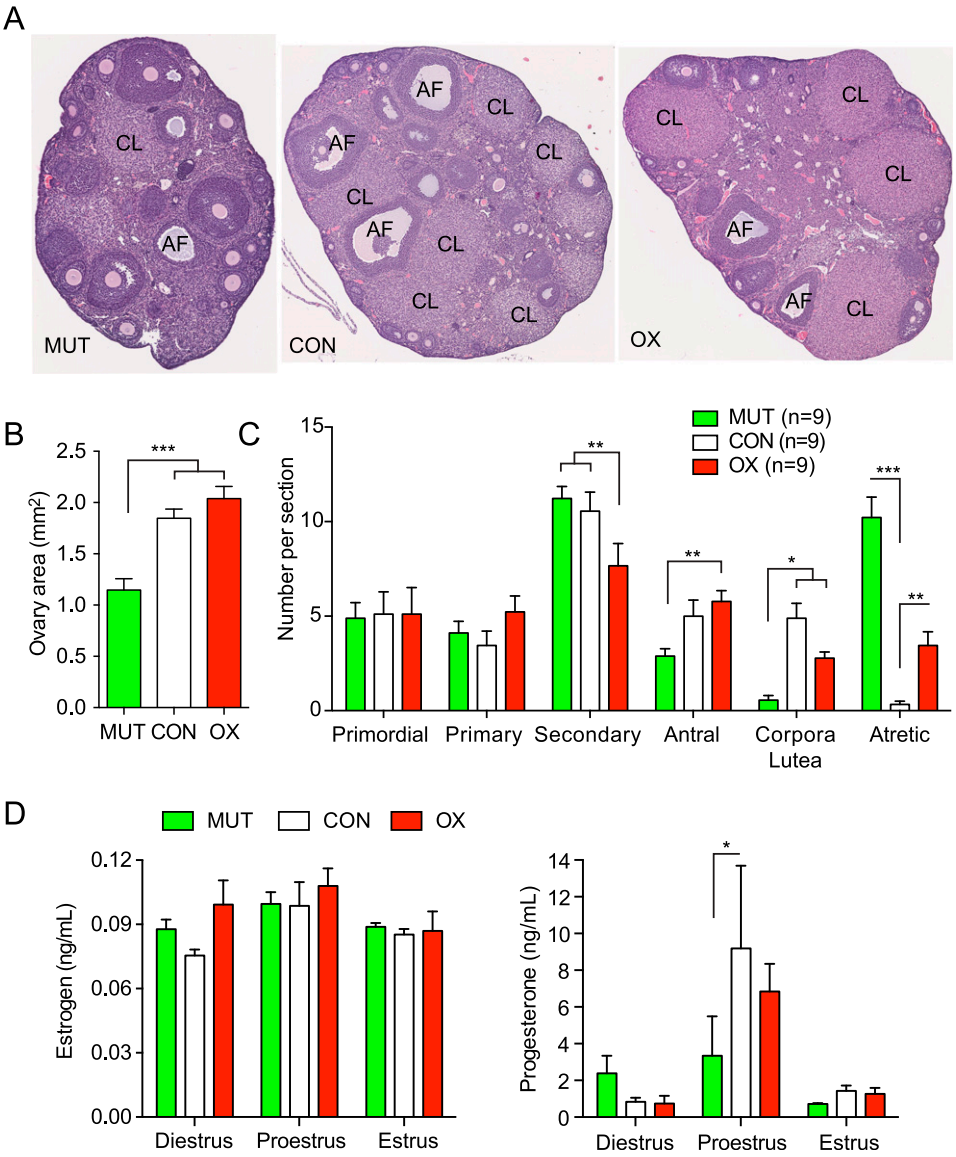

Figure 6. SIRT1 inactivation reduces ovary size and number of corpora lutea. OX mice are in red, CON mice in white, and MUT mice in green. (A) Ovarian morphology. Representative hematoxylin and eosin stained sections of ovaries obtained at euthanasia. (B) Quantification of ovarian cross-sectional area for MUT (n = 9), CON (n = 35), and OX (n = 9) ovaries. (C) Quantification of follicle stage and corpora lutea. Number of follicles at each stage per section for MUT (n = 9), CON (n = 9), and OX (n = 9) mice. (D) Estrogen and progesterone levels during diestrus, proestrus, and estrus. Data are shown as mean ± SEM. Asterisks indicate significance by *post hoc* testing. $*P < 0.05$; $**P < 0.01$; $***P < 0.001$. AF, antral follicle; CL, corpora lutea.

Additionally, we observed that overexpression of wild-type SIRT1 in neurons in either female or male mice impaired glucose tolerance, which is consistent with the improved glucose tolerance in the deacetylase-inactive mutant mice, but it did not have a major effect on food intake (50). Consistent with a role for SIRT1 in the response to caloric restriction, neuronal overexpression of SIRT1 rendered the mice more sensitive to the metabolic effects of caloric restriction. In contrast to those results, in this study we found that genetic manipulation of SIRT1 in astrocytes altered feeding behavior, with loss of SIRT1 enzyme activity decreasing food intake and SIRT1 overexpression increasing food intake in both males and females, which was unrelated to leptin. This effect resulted in significant differences in body weight and significant differences in glucose tolerance, although we do not believe that the altered glucose tolerance simply reflected the differences in body weight, because the differences persisted if weight-matched subgroups were compared. The more glucose-tolerant MUT mice had lower FBG and lower FI, leading to a lower HOMA-IR that agreed with the improved glucose tolerance. The glucose tolerance with SIRT1 overexpression or inactivation in astrocytes was consistent with the GTT effects seen in neurons, but the alterations in insulin tolerance in the astrocyte SIRT1 mice were not observed in the neuronal mutants (50). The insulin tolerance was paradoxical given the GTTs. This effect may be related to

altered insulin clearance, because C-peptide levels were not changed, indicating that insulin secretion was normal. During metabolic testing, the OX mice were more active, generated more heat but had a lower VO_2 than the MUT mice, suggesting more energy consumption but less efficient fuel utilization. Food intake was not different between genotypes in the singly housed metabolic cage study, but the overexpressing mice ate more food under normal housing conditions (nearly twice as much for females) that probably compensated for the greater energy consumption and allowed greater weight gain. Astrocytic SIRT1, unlike neuronal SIRT1, did not appear to influence the response to fasting.

How do astrocytes contribute to metabolic regulation? Astrocytes play an essential role in the deliverance of glucose, oxygen, and other nutrients to neurons (31, 51, 52). Astrocyte signaling via IKK/NF-κB is necessary for DIO and hypothalamic inflammation and for increased food intake during acute high-fat feeding (39, 53). Astrocytes can also control food intake by depressing ghrelin-evoked hyperphagia but facilitating leptin-induced anorexia, by inhibiting *Agrp* neurons (54). As a result, mice lacking the leptin receptor in astrocytes are hyperphagic and gain more weight on HFDs (38, 55), whereas mice lacking the insulin receptor in astrocytes are metabolically normal but prone to anxiety and depressive-like behavior (56). How is SIRT1 linked to these astrocytic pathways? SIRT1 has been suggested to impair NF-κB signaling in the hypothalamus (57), and astrocyte NF-κB signaling is necessary for DIO (39). Consistent with this model, expression of the deacetylase-deficient SIRT1 mutant protected female mice from DIO, whereas SIRT1 overexpression increased DIO. We observed increases in hypothalamic *Il6* and *Tnfa* expression, particularly in the SIRT1-overexpressing mice, which would be consistent with the glucose intolerant phenotype. Thus SIRT1 in astrocytes could play a role in feeding behavior and glucose metabolism through such mechanisms, but further studies will be needed to dissect the pathways involved.

At the female reproductive level, overexpression of SIRT1 increased the number of estrous cycles, increased time in diestrus, and decreased time in estrus. A greater proportion of overexpressing mice showed LH surges, whereas only one deacetylase-deficient mouse showed an LH surge. The SIRT1-deficient mice also showed reduced corpora lutea upon examination of the ovaries, which is consistent with decreased ovulation. These mice also did not show any changes in FSH levels throughout the estrous cycle that may explain the lack of progression into the next follicular cycle. Hypothalamic *Kiss1* levels were reduced in the deacetylase-deficient SIRT1 mice, but the GnRH neurons showed a normal response to exogenous kisspeptin-10, indicating that the defect probably lies upstream of the GnRH neuron, either at the *Kiss1* neurons or further upstream. Whether or how astrocytes influence *Kiss1* neurons is not known but warrants further investigation. In summary, SIRT1 in astrocytes has divergent effects to impair glucose metabolism and increase sensitivity to DIO in females but to improve reproductive function by increasing the frequency of LH surges and ovulation.

Acknowledgments

We acknowledge the assistance of the Histology Core at the Moores' Cancer Center and the Genomics Core at the Sanford Consortium for Regenerative Medicine.

Financial Support: This work is funded in part by National Institutes of Health (NIH) grants to N.J.G.W. (HD012303, CA155435, CA196853) and a VA Merit Review award to N.J.G.W. (I01BX000130). The Histology Core at the Moores' Cancer Center is supported by NIH Grant CA023100.

Current Affiliation: E. Rickert's current affiliation is BioMendics, LLC, Rootstown, Ohio 44272. M. Fernandez's current affiliation is the Laboratory of Neuroendocrinology, Instituto de Biología y Medicina Experimental, CONICET, C1428ADN Buenos Aires, Argentina.

Correspondence: Nicholas J. G. Webster, PhD, Department of Medicine, University of California, San Diego, 9500 Gilman Drive, La Jolla, California 92093. E-mail: nwebster@ucsd.edu.

Disclosure Summary: The authors have nothing to disclose.

References and Notes

1. Haigis MC, Sinclair DA. Mammalian sirtuins: biological insights and disease relevance. *Annu Rev Pathol*. 2010;**5**(1):253–295.
2. McBurney MW, Clark-Knowles KV, Caron AZ, Gray DA. SIRT1 is a highly networked protein that mediates the adaptation to chronic physiological stress. *Genes Cancer*. 2013;**4**(3-4):125–134.
3. Chang HC, Guarente L. SIRT1 and other sirtuins in metabolism. *Trends Endocrinol Metab*. 2014;**25**(3):138–145.
4. Schenk S, McCurdy CE, Philp A, Chen MZ, Holliday MJ, Bandyopadhyay GK, Osborn O, Baar K, Olefsky JM. Sirt1 enhances skeletal muscle insulin sensitivity in mice during caloric restriction. *J Clin Invest*. 2011;**121**(11):4281–4288.
5. Pfluger PT, Herranz D, Velasco-Miguel S, Serrano M, Tschöp MH. Sirt1 protects against high-fat diet-induced metabolic damage. *Proc Natl Acad Sci USA*. 2008;**105**(28):9793–9798.
6. Boutant M, Cantó C. SIRT1: a novel guardian of brown fat against metabolic damage. *Obesity (Silver Spring)*. 2016;**24**(3):554.
7. Cheng HL, Mostoslavsky R, Saito S, Manis JP, Gu Y, Patel P, Bronson R, Appella E, Alt FW, Chua KF. Developmental defects and p53 hyperacetylation in Sir2 homolog (SIRT1)-deficient mice. *Proc Natl Acad Sci USA*. 2003;**100**(19):10794–10799.
8. McBurney MW, Yang X, Jardine K, Hixon M, Boekelheide K, Webb JR, Lansdorp PM, Lemieux M. The mammalian SIR2alpha protein has a role in embryogenesis and gametogenesis. *Mol Cell Biol*. 2003;**23**(1):38–54.
9. Wang RH, Sengupta K, Li C, Kim HS, Cao L, Xiao C, Kim S, Xu X, Zheng Y, Chilton B, Jia R, Zheng ZM, Appella E, Wang XW, Ried T, Deng CX. Impaired DNA damage response, genome instability, and tumorigenesis in SIRT1 mutant mice. *Cancer Cell*. 2008;**14**(4):312–323.

10. Seifert EL, Caron AZ, Morin K, Coulombe J, He XH, Jardine K, Dewar-Darch D, Boekelheide K, Harper ME, McBurney MW. SirT1 catalytic activity is required for male fertility and metabolic homeostasis in mice. *FASEB J*. 2012;**26**(2):555–566.
11. Ding RB, Bao J, Deng CX. Emerging roles of SIRT1 in fatty liver diseases. *Int J Biol Sci*. 2017;**13**(7):852–867.
12. Xu F, Gao Z, Zhang J, Rivera CA, Yin J, Weng J, Ye J. Lack of SIRT1 (Mammalian Sirtuin 1) activity leads to liver steatosis in the SIRT1+/− mice: a role of lipid mobilization and inflammation. *Endocrinology*. 2010;**151**(6):2504–2514.
13. Couzinet B, Young J, Brailly S, Le Bouc Y, Chanson P, Schaison G. Functional hypothalamic amenorrhoea: a partial and reversible gonadotrophin deficiency of nutritional origin. *Clin Endocrinol (Oxf)*. 1999;**50**(2):229–235.
14. Allaway HC, Southmayd EA, De Souza MJ. The physiology of functional hypothalamic amenorrhea associated with energy deficiency in exercising women and in women with anorexia nervosa. *Horm Mol Biol Clin Investig*. 2016;**25**(2):91–119.
15. Bell EL, Nagamori I, Williams EO, Del Rosario AM, Bryson BD, Watson N, White FM, Sassone-Corsi P, Guarente L. SirT1 is required in the male germ cell for differentiation and fecundity in mice. *Development*. 2014;**141**(18):3495–3504.
16. Kolthur-Seetharam U, Teerds K, de Rooij DG, Wendling O, McBurney M, Sassone-Corsi P, Davidson I. The histone deacetylase SIRT1 controls male fertility in mice through regulation of hypothalamic-pituitary gonadotropin signaling. *Biol Reprod*. 2009;**80**(2):384–391.
17. Tatone C, Di Emidio G, Vitti M, Di Carlo M, Santini S, Jr, D'Alessandro AM, Falone S, Amicarelli F. Sirtuin functions in female fertility: possible role in oxidative stress and aging. *Oxid Med Cell Longev*. 2015;**2015**:659687.
18. Herskovits AZ, Guarente L. SIRT1 in neurodevelopment and brain senescence. *Neuron*. 2014;**81**(3):471–483.
19. Abe-Higuchi N, Uchida S, Yamagata H, Higuchi F, Hobara T, Hara K, Kobayashi A, Watanabe Y. Hippocampal Sirtuin 1 signaling mediates depression-like behavior. *Biol Psychiatry*. 2016;**80**(11):815–826.
20. Albani D, Polito L, Forloni G. Sirtuins as novel targets for Alzheimer's disease and other neurodegenerative disorders: experimental and genetic evidence. *J Alzheimers Dis*. 2010;**19**(1):11–26.
21. Libert S, Pointer K, Bell EL, Das A, Cohen DE, Asara JM, Kapur K, Bergmann S, Preisig M, Otowa T, Kendler KS, Chen X, Hettema JM, van den Oord EJ, Rubio JP, Guarente L. SIRT1 activates MAO-A in the brain to mediate anxiety and exploratory drive. *Cell*. 2011;**147**(7):1459–1472.
22. Michán S, Li Y, Chou MM, Parrella E, Ge H, Long JM, Allard JS, Lewis K, Miller M, Xu W, Mervis RF, Chen J, Guerin KI, Smith LE, McBurney MW, Sinclair DA, Baudry M, de Cabo R, Longo VD. SIRT1 is essential for normal cognitive function and synaptic plasticity. *J Neurosci*. 2010;**30**(29):9695–9707.
23. Boily G, Seifert EL, Bevilacqua L, He XH, Sabourin G, Estey C, Moffat C, Crawford S, Saliba S, Jardine K, Xuan J, Evans M, Harper ME, McBurney MW. SirT1 regulates energy metabolism and response to caloric restriction in mice. *PLoS One*. 2008;**3**(3):e1759.
24. Cohen DE, Supinski AM, Bonkowski MS, Donmez G, Guarente LP. Neuronal SIRT1 regulates endocrine and behavioral responses to calorie restriction. *Genes Dev*. 2009;**23**(24):2812–2817.
25. Satoh A, Brace CS, Ben-Josef G, West T, Wozniak DF, Holtzman DM, Herzog ED, Imai S. SIRT1 promotes the central adaptive response to diet restriction through activation of the dorsomedial and lateral nuclei of the hypothalamus. *J Neurosci*. 2010;**30**(30):10220–10232.
26. Rickert E, Fernandez MO, Choi I, Gorman M, Olefsky JM, Webster NJG. Neuronal SIRT1 regulates metabolic and reproductive function and the response to caloric restriction. *J Endocr Soc*. 2018;**3**(2):427–445.
27. Ramadori G, Fujikawa T, Fukuda M, Anderson J, Morgan DA, Mostoslavsky R, Stuart RC, Perello M, Vianna CR, Nillni EA, Rahmouni K, Coppari R. SIRT1 deacetylase in POMC neurons is required for homeostatic defenses against diet-induced obesity. *Cell Metab*. 2010;**12**(1):78–87.
28. Dietrich MO, Antunes C, Geliang G, Liu ZW, Borok E, Nie Y, Xu AW, Souza DO, Gao Q, Diano S, Gao XB, Horvath TL. Agrp neurons mediate Sirt1's action on the melanocortin system and energy balance: roles for Sirt1 in neuronal firing and synaptic plasticity. *J Neurosci*. 2010;**30**(35):11815–11825.
29. Sasaki T, Kikuchi O, Shimpuku M, Susanti VY, Yokota-Hashimoto H, Taguchi R, Shibusawa N, Sato T, Tang L, Amano K, Kitazumi T, Kuroko M, Fujita Y, Maruyama J, Lee YS, Kobayashi M, Nakagawa T, Minokoshi Y, Harada A, Yamada M, Kitamura T. Hypothalamic SIRT1 prevents age-associated weight gain by improving leptin sensitivity in mice. *Diabetologia*. 2014;**57**(4):819–831.
30. Ramadori G, Fujikawa T, Anderson J, Berglund ED, Frazao R, Michán S, Vianna CR, Sinclair DA, Elias CF, Coppari R. SIRT1 deacetylase in SF1 neurons protects against metabolic imbalance. *Cell Metab*. 2011;**14**(3):301–312.
31. Douglass JD, Dorfman MD, Thaler JP. Glia: silent partners in energy homeostasis and obesity pathogenesis. *Diabetologia*. 2017;**60**(2):226–236.
32. Hill JW, Elmquist JK, Elias CF. Hypothalamic pathways linking energy balance and reproduction. *Am J Physiol Endocrinol Metab*. 2008;**294**(5):E827–E832.
33. Roh E, Kim MS. Brain regulation of energy metabolism. *Endocrinol Metab (Seoul)*. 2016;**31**(4):519–524.
34. Barreto GE, Gonzalez J, Torres Y, Morales L. Astrocytic-neuronal crosstalk: implications for neuroprotection from brain injury. *Neurosci Res*. 2011;**71**(2):107–113.
35. Magistretti PJ. Neuron-glia metabolic coupling and plasticity. *Exp Physiol*. 2011;**96**(4):407–410.
36. Newman EA. New roles for astrocytes: regulation of synaptic transmission. *Trends Neurosci*. 2003;**26**(10):536–542.
37. García-Cáceres C, Quarta C, Varela L, Gao Y, Gruber T, Legutko B, Jastroch M, Johansson P, Ninkovic J, Yi CX, Le Thuc O, Szigeti-Buck K, Cai W, Meyer CW, Pfluger PT, Fernandez AM, Luquet S, Woods SC, Torres-Alemán I, Kahn CR, Götz M, Horvath TL, Tschöp MH. Astrocytic insulin signaling couples brain glucose uptake with nutrient availability. *Cell*. 2016;**166**(4):867–880.
38. Wang Y, Hsuchou H, He Y, Kastin AJ, Pan W. Role of astrocytes in leptin signaling. *J Mol Neurosci*. 2015;**56**(4):829–839.
39. Douglass JD, Dorfman MD, Fasnacht R, Shaffer LD, Thaler JP. Astrocyte IKKβ/NF-κB signaling is required for diet-induced obesity and hypothalamic inflammation. *Mol Metab*. 2017;**6**(4):366–373.
40. Fernandez MO, Hsueh K, Park HT, Sauceda C, Hwang V, Kumar D, Kim S, Rickert E, Mahata S, Webster NJG. Astrocyte-specific deletion of peroxisome-proliferator activated receptor-γ impairs glucose metabolism and estrous cycling in female mice. *J Endocr Soc*. 2017;**1**(11):1332–1350.
41. Ducret E, Anderson GM, Herbison AE. RFamide-related peptide-3, a mammalian gonadotropin-inhibitory hormone ortholog, regulates gonadotropin-releasing hormone neuron firing in the mouse. *Endocrinology*. 2009;**150**(6):2799–2804.
42. Ferris JK, Tse MT, Hamson DK, Taves MD, Ma C, McGuire N, Arckens L, Bentley GE, Galea LA, Floresco SB, Soma KK. Neuronal gonadotrophin-releasing hormone (GnRH) and astrocytic gonadotrophin inhibitory hormone (GnIH) immunoreactivity in the adult rat hippocampus. *J Neuroendocrinol*. 2015;**27**(10):772–786.
43. Shimizu M, Bédécarrats GY. Activation of the chicken gonadotropin-inhibitory hormone receptor reduces gonadotropin releasing hormone receptor signaling. *Gen Comp Endocrinol*. 2010;**167**(2):331–337.

44. Tsutsui K, Bentley GE, Bedecarrats G, Osugi T, Ubuka T, Kriegsfeld LJ. Gonadotropin-inhibitory hormone (GnIH) and its control of central and peripheral reproductive function. *Front Neuroendocrinol*. 2010;**31**(3):284–295.
45. Prevot V, Bellefontaine N, Baroncini M, Sharif A, Hanchate NK, Parkash J, Campagne C, de Seranno S. Gonadotrophin-releasing hormone nerve terminals, tanycytes and neurohaemal junction remodelling in the adult median eminence: functional consequences for reproduction and dynamic role of vascular endothelial cells. *J Neuroendocrinol*. 2010;**22**(7):639–649.
46. Prevot V, Hanchate NK, Bellefontaine N, Sharif A, Parkash J, Estrella C, Allet C, de Seranno S, Campagne C, de Tassigny X, Baroncini M. Function-related structural plasticity of the GnRH system: a role for neuronal-glial-endothelial interactions. *Front Neuroendocrinol*. 2010;**31**(3):241–258.
47. Rodríguez EM, Blázquez JL, Pastor FE, Peláez B, Peña P, Peruzzo B, Amat P. Hypothalamic tanycytes: a key component of brain-endocrine interaction. *Int Rev Cytol*. 2005;**247**: 89–164.
48. Choi I, Rickert E, Fernandez M, Webster NJG. Data from: SIRT1 in astrocytes regulates glucose metabolism and reproductive function. figshare 2019. Deposited 16 April 2019. https://dx.doi.org/10.6084/m9.figshare.7999538.
49. Myers M, Britt KL, Wreford NG, Ebling FJ, Kerr JB. Methods for quantifying follicular numbers within the mouse ovary. *Reproduction*. 2004;**127**(5):569–580.
50. Lu M, Sarruf DA, Li P, Osborn O, Sanchez-Alavez M, Talukdar S, Chen A, Bandyopadhyay G, Xu J, Morinaga H, Dines K, Watkins S, Kaiyala K, Schwartz MW, Olefsky JM. Neuronal Sirt1 deficiency increases insulin sensitivity in both brain and peripheral tissues. *J Biol Chem*. 2013;**288**(15):10722–10735.
51. Chowen JA, Argente-Arizón P, Freire-Regatillo A, Frago LM, Horvath TL, Argente J. The role of astrocytes in the hypothalamic response and adaptation to metabolic signals. *Prog Neurobiol*. 2016;**144**:68–87.
52. Yi CX, Habegger KM, Chowen JA, Stern J, Tschöp MH. A role for astrocytes in the central control of metabolism. *Neuroendocrinology*. 2011;**93**(3):143–149.
53. Buckman LB, Thompson MM, Lippert RN, Blackwell TS, Yull FE, Ellacott KL. Evidence for a novel functional role of astrocytes in the acute homeostatic response to high-fat diet intake in mice. *Mol Metab*. 2014;**4**(1):58–63.
54. Yang L, Qi Y, Yang Y. Astrocytes control food intake by inhibiting AGRP neuron activity via adenosine A1 receptors. *Cell Reports*. 2015;**11**(5):798–807.
55. Kim JG, Suyama S, Koch M, Jin S, Argente-Arizon P, Argente J, Liu ZW, Zimmer MR, Jeong JK, Szigeti-Buck K, Gao Y, Garcia-Caceres C, Yi CX, Salmaso N, Vaccarino FM, Chowen J, Diano S, Dietrich MO, Tschöp MH, Horvath TL. Leptin signaling in astrocytes regulates hypothalamic neuronal circuits and feeding. *Nat Neurosci*. 2014;**17**(7):908–910.
56. Cai W, Xue C, Sakaguchi M, Konishi M, Shirazian A, Ferris HA, Li ME, Yu R, Kleinridders A, Pothos EN, Kahn CR. Insulin regulates astrocyte gliotransmission and modulates behavior. *J Clin Invest*. 2018;**128**(7):2914–2926.
57. Zhou X, Zhang H, He L, Wu X, Yin Y. Long-term l-serine administration reduces food intake and improves oxidative stress and Sirt1/NFκB signaling in the hypothalamus of aging mice. *Front Endocrinol (Lausanne)*. 2018;**9**:476.